EUROPEAN TRANSACTIONS ON ELECTRICAL POWER
Euro. Trans. Electr. Power 2006; **16**:297–310
Published online 2 February 2006 in Wiley InterScience (www.interscience.wiley.com). DOI: 10.1002/etep.88

Acoustic noise generated by air power reactor in open-air substation

Jean-Louis Lilien*,†

Montefiore Electrical Institute. University of Liège, B-4000 Liège, Belgium

SUMMARY

Air power reactors are often used in substations for different purposes such as fault current limiter, reactive power consumption, harmonic filtering, and grounding impedance. They are also used in test laboratories for electric material testing. If the basic design is in relation with its electric duties, the design rules also include some restrictions for thermodynamics, structural dynamics, and acoustics. The full interaction between these four engineering fields is particularly important for acoustic noise produced by the reactor. This noise level is limited by international rules. The aim of this paper is to present a simple analytical method to evaluate the acoustics of such air power reactors and to compare such a method with more sophisticated numerical evaluations. Last but not least, some trends in noise control methods are described. Detailed tests results are presented for validation of the proposed method to properly evaluate the acoustics of single core reactors. Copyright © 2006 John Wiley & Sons, Ltd.

KEY WORDS: power substation; air reactor; acoustics; electromagnetics; structural dynamics; acoustic noise.

1. INTRODUCTION AND HYPOTHESIS.

Figure 1 shows a single core reactor that has been tested in this project. The aim of this paper is not to detail the electric design of the reactor (reactive power level needed, withstanding overvoltages, appropriate conductor cross sections, number of wires in parallel, number of turns, material used—single or multi-layer conductor, diameter and height of the structure, etc.). In the case of a short-circuit (not treated in this paper), very strong design forces, including torsion forced by the spiders, must be taken into account in the design. These cases must include asymmetry of the current, which is not the case in this paper, where only nominal current is taken into account. Our present goal is to evaluate the acoustic emissions.

In permanence, several tenths of amperes generate a magnetic field applied on the wires, which induces electromagnetic forces whose frequency is double that of the current. Let us recall that the force is orthogonal to both current and magnetic fields.

This kind of solenoid can be subjected to strong harmonic currents, all of these inducing pulsating forces (one continuous component and one alternative one at double the current frequency).

*Correspondence to: Jean-Louis Lilien, Montefiore Electrical Institute. University of Liège, B-4000 Liège, Belgium
†E-mail: Lilien@montefiore.ulg.ac.be

Contract/grant sponsor: Région Wallonne de Belgique; contract/grant number: 3777.

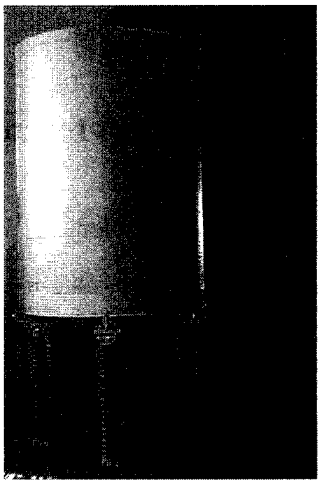

Figure 1. One-phase air reactor for neutral to ground connection. 132 kVar, 100 kV isolation (neutral), 345 turns with 70 A_{rms}, inductance 86 mH, Diameter 1.2 m, core height 1.4 m.

This paper is focused on one fundamental frequency 50 Hz, creating 100 Hz pulsating forces.

The pulsating forces will produce vibrations both in radial and axial directions (axial forces due to the inclination of magnetic field directions near the core ends).

Moreover, the current input and output are generally done through spiders (one on the top, one on the bottom of the cylinder, Figure 2), and there are also forces acting on these spiders, both by direct action of the magnetic field created by the solenoid onto the spider current and by inertial forces due to the axial movement of the reactor.

All vibrating parts induce acoustic noise, at 100 Hz for our basic case. It must be noted that the noise is generated by very small movements of the core. It is a fact that more than 40 dBA at 100 Hz could be induced at 2 m, far from the reactor with a limited 0.02 mm/second vibration speed (amplitude is thus 0.03 micron). (Such a value was due to a nominal current of 70 A).

The reactor is of course insulated from the ground by insulators. For our application, these insulators had a basic 78 Hz frequency and a cantilever stiffness of 10^6 N/m. The whole structure mounted on its

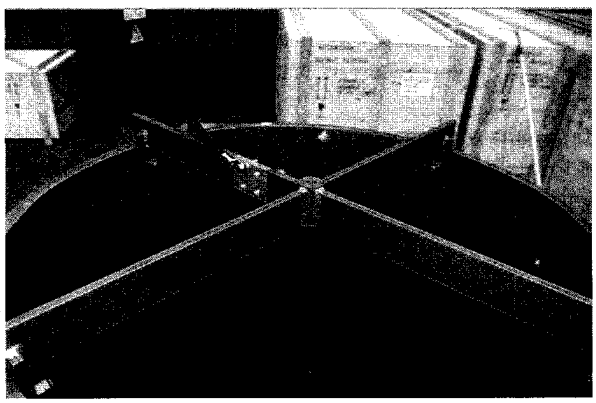

Figure 2. The superior spider with input current connection.

four insulators has many frequencies and modal shapes. Some of these could be close to excitation forces. We clearly need a structural dynamic analysis.

The reactor looks like a cylinder with two open ends, and such a structure also has acoustic resonances for some frequencies. Moreover, the inner part of the wall cylinder is oscillating in opposite phase with the external part (because it is the same wall!). Does this have any effect on the noise produced at a certain distance from the reactor? Does this effect have any compensation due to phase-shift motion of walls, in particular what could happen in a three-phase arrangement?

Some other problems, not detailed here, should also be mentioned:

- Nominal temperature of the core is generally close to 40–80°C, which could have effects on the wall texture, with regard to its damping properties as well as acoustic absorption.
- Such a power reactor will also induce a strong magnetic field in its vicinity, creating an EMC problem. (The field is more than 1000 times those existing on the ground close to an EHV overhead line loaded at its nominal value).

2. ELECTROMAGNETICS AND WALL SPEED EVALUATION

To evaluate the magnetic field inside a solenoid is not a problem using Ampere's law. But in fact we need the field on the wires to evaluate forces. Numerical simulation can be performed, as shown by the result on Figure 3.

We have developed a simple method to properly evaluate the field on the wires themselves all along the reactor. Similar developments have also been realized to evaluate the magnetic field acting on the spiders.

Evaluation of the forces is performed as follows:

The electromagnetic field inside the single core reactor is evaluated as a function of time t. If R is the radius of the cylinder (m), ω the current pulsation (rad/second), H the total height of the reactor (m), N the number of turns per unit length, I_{rms} the root mean square value of the sinusoidal $i(t)$ current (A), nbr the total number of turns, ϕ the mean thickness of one turn, and μ_0 the vacuum magnetic permeability (H/m), the following mean value can be achieved in the center of the reactor:

$$B(t) = \frac{N}{H}\left(\left(R^2 + H^2\right)^{0,5} - R\right)\mu_0 i(t) \tag{1}$$

The actual axial induction magnetic field on the conductor is z-dependent and can be evaluated using the theory of solenoid; it is a similar expression with an additional constant factor. For the sake of simplicity, we will suppose independence of z.

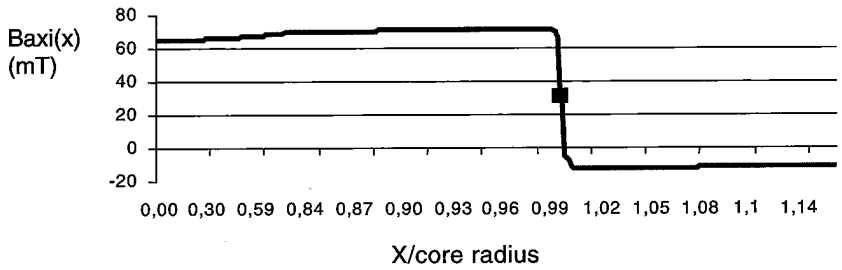

Figure 3. Peak axial magnetic field (for 200 A_{rms}). The square dot indicates the value on the aluminium wire. The field is computed at mid-height of the power reactor.

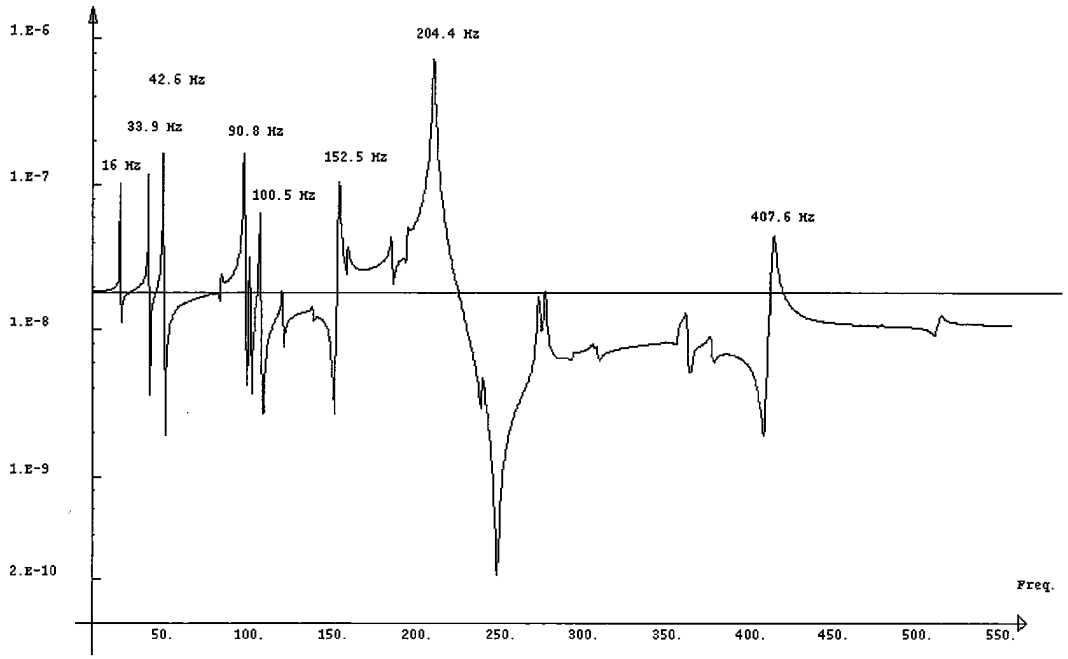

Figure 5. Frequency response of the displacement of point A (Figure 4) of the reactor submitted to actual sinusoidal forced excitation on the core and the spider as in a real situation.

The measured speeds are in the range 5–10 times the evaluated ones by quasi-steady theory, but are not uniformly distributed. We have had no clear explanation of these results up to now because such measured speed would have produced a much higher noise than that measured during the same test. The hypothesis maintained in this paper is that the deformation shown on Figure 6, and actually measured, is not entirely due to structural dynamics. A tentative qualitative explanation is presented

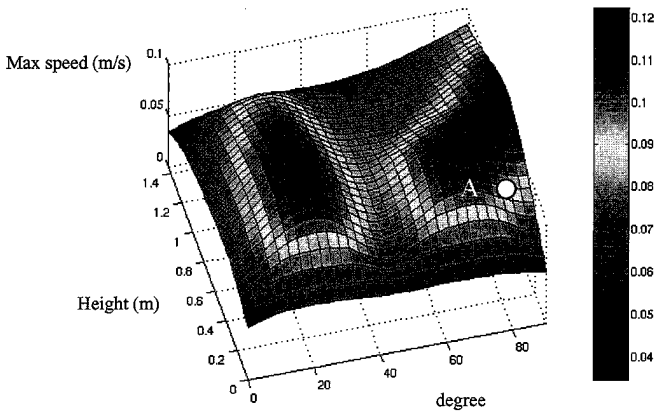

Figure 6. Hundred hertz wall speed on a quarter of the apparatus (measured by laser vibrometry during full scale testing) 0° and 90° are the locations of spider connection. Right scale in m/second.

here after. At this stage we emphasize that we were particularly astonished by Figure 6, which showed the higher speed close to one spider location (at 90°).

4. ACOUSTICS

With the basic hypothesis of incompressible fluid (air), the acoustics can be evaluated by solving the well-known equation valid for sinusoidal pressure variation (at a pulsation ω): [3]

$$\Delta p = -\frac{\omega^2}{c^2} p \tag{5}$$

and for boundary conditions (using the wall speed v):

$$\omega \times \rho \times v = -\text{grad}(p) \tag{6}$$

the pressure normal gradient being null on the ground. Δ is the Laplacian operator. Where p is pressure (Pa), c the sound speed (340 m/second in standard conditions), ρ the volumetric mass of air (about 1.2 kg/m^3), ω the pulsation (rad/second) of the speed v (m/second) (three components, only normal v_{rad} (Equation 4) component exists on the reactor wall and is null on the ground).

With a given pressure distribution, a given wall speed profile and time evolution (phase shift, frequency, amplitude), the use of calculation can give access separately to the noise generated by the inner wall of the cylinder (case A, Figure 7), the one generated by the external wall (case B, Figure 8) and the real case of both combined together (case C, Figure 9), as well as a global response in the frequency domain (Figure 10).

These calculations have been performed for a maximum wall speed of 0.2 mm/second at 100 Hz and 1 mm/second at 500 Hz, corresponding to the same quasi-steady displacement.

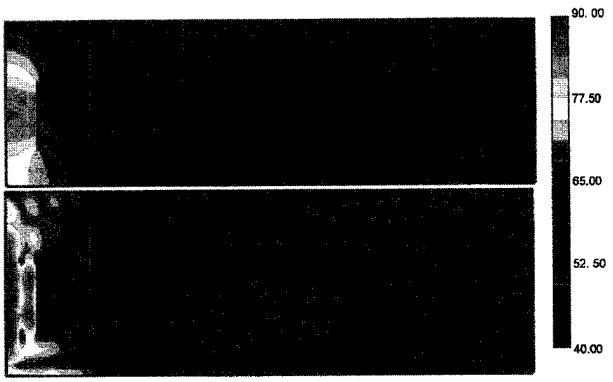

Figure 7. Noise (dB) generated by inner wall movement only (case A). There is acoustic resonance inside the cylinder. Upper case at 100 Hz, second case at 500 Hz. Left-hand side vertical border is the axis of symmetry. The cylinder wall can be clearly seen on Figure 10, and is of course located similarly on the other figures (reduced to a small rectangle due to axi-symmetricview). Right scale in dB.

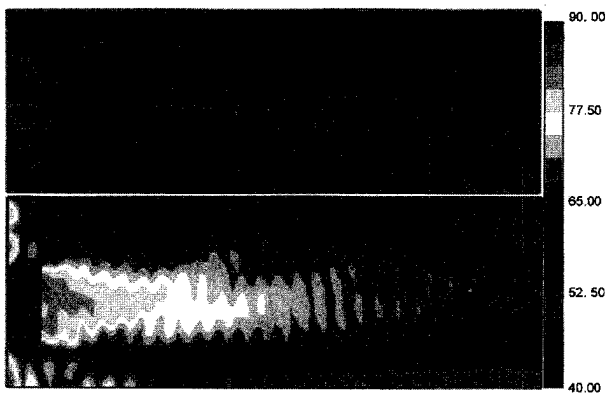

Figure 8. Noise (dB) generated by external wall only (case B) (moving in phase opposition with case A). Upper case at 100 Hz, second case at 500 Hz.

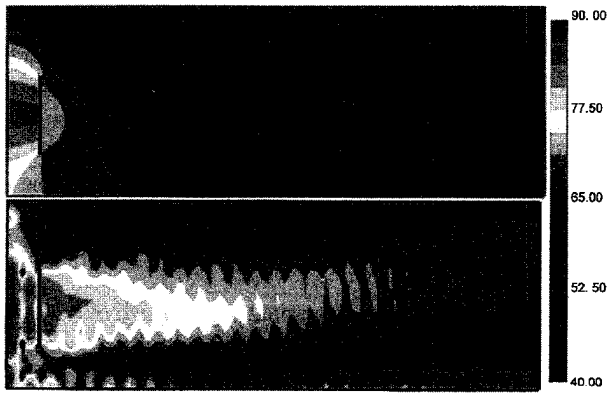

Figure 9. Noise (dB) generated by case A and B together. Upper case at 100 Hz, second case at 500 Hz (case C).

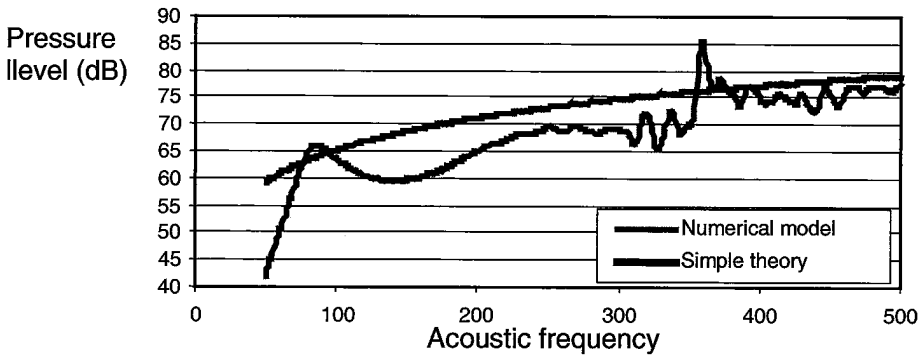

Figure 10. Frequency response of pressure level (in dB) at 3 m from the reactor, for a cylinder similar to our reactor and placed at about 1 m from the ground in the semi-infinite space. Resonances at 85 and 360 Hz.

The input acoustic power is given by (depending on wall normal speed v_{rad}, from Equation 4):

$$W_{input} = \frac{\rho c}{2} \int_{Cylinder} |v_{rad}|^2 dS \tag{7}$$

The output acoustic power depends on air particle speed v_n near surface emission (oriented in pressure gradient, following Equation 6) and is given by:

$$W_{output} = \frac{1}{2} \int_{Cylinder} p v_n^* dS = \frac{1}{2} \int_{internal(A)+external(B)faces} (p_A + p_B) \cdot v_n^* \, dS \tag{8}$$

where A and B are the cases detailed on Figures 7 and 8.

The difference between input and output power very much depends on surface emission efficiency (= radiation ratio) and on phase shift between induced pressures (compensation may occur for out of phase variation f.e.). Numerical evaluations are given in Table 1.

It is amazing to observe that the noise mainly comes from the inner wall movement at 100 Hz (wavelength 3.4 m), and more obviously mainly from the outer wall at 500 Hz (wavelength 0.7 m). The case at 100 Hz is of course related to acoustic resonance, creating two synchronous noise sources (due to axial resonance), which interfere with each other at a 45° destructive area, which can be seen on Figures 7 and 8 (upper part). This phenomenon is in relation with specific relation between the volume of air inside the cylinder and with the wavelength of excitation (100 Hz at a speed of about 340 m/second give a wavelength of 3.4 m). For the 500 Hz, the resonance is radial. A frequency response of pressure level at 3 m far from the reactor is given on Figure 10. This figure points out typical acoustic local resonance, for this case around 85 and 360 Hz.

On the same figure, the theory developed in this paper is reproduced (Equation 4 combined with Equations 9 and 10), which neglect these resonances. Our theory supposes a perfectly reflective wall and ground (no absorption), and a unity factor for efficiency of noise emissions from both inner and outer walls.

From both acoustic theory and these results, one can clearly make the following conclusions:

- The noise generated by the inner and external walls can be combined (adding pressures) with a very limited effect of phase shift at 'high' frequencies (a frequency-dependent correction factor has been introduced for lower ones). Ground reflection may double the contribution (image theory), if it is perfectly reflective.
- The cylinder with two open ends has a resonant frequency depending mainly on its height and diameter. In this case, it is unfortunately close to 100 Hz, as can be seen on Figures 7 and 10. Due to that, most of the noise, even outside the cylinder is due to inner wall movement, but this is not generally the case.

Table I. Emission efficiencies and acoustic power generated (input) and emitted (output) for two different frequencies (cf. Figures 8–10) (courtesy FFT).

	Case A inner wall	Case B outer wall	Case C both walls	Total input power (10^{-6} W)	Active output power (10^{-6} W)
100 Hz	2.2	0.6	2.1	77	162
500 Hz	0.08	0.9	0.49	1927	937

- The quasi-steady theory combined with a unity factor of emission efficiency produce a curve which is valid outside the resonance area most of the time with safety values, because the hypothesis of a unity factor of emission is dramatic, except in the resonance area.

From these hypotheses and observations, we can evaluate the noise generated by the following equations:

We introduce the wall speed (Equation 4, limited to rms) into the evaluation of acoustic power generated by the reactor (Equation 7):

$$W = \rho \times c \times v_{\text{rms}}^2 \times S_{\text{emission}} \quad \text{(Watts)} \tag{9}$$

where S_{emission} is the wall surface (external + internal). The air particle speeds are supposed to be identical for output power and in phase with pressure variation.

The noise at a given location is finally given by the pressure at that location, which can be deduced from the following formula, (cylindrical propagation, valid for short distances like 2 m):

$$p^2 = \frac{\rho \times c \times W}{S_{\text{propagation}}} \quad (\text{Pa})^2 \tag{10}$$

Generally we consider only rms value of pressure and we convert it to dBA which is a well-known correction used from dB to adapt sound pressure to ear receptivity (that correction is frequency-dependent).

Formula 10, together with Equations 9 and 4 give access to the main factors that influence noise.

5. DIRECTIONAL EFFECTS

During measurement it was clear (some figures will be shown below) that a directional effect occurred, which obviously was not detected with the first theory (a symmetric structure with distributed pressure inside would have produced no directional effect). Such an effect could also explain velocity measurements (Figure 6) where we can see a maximum velocity at a point *fixed* by the spiders!

Such an observation makes us think about asymmetric effects. As the supporting insulators are not submitted to any force or bending torque (all forces acting on the reactor are internal forces), the only dissymmetry could come from dynamics. Figure 4 gives access, at 100 Hz, to the reactor shape, showing in and out of phase movements and different shapes around the reactor.

This effect is dependent on the frequency of excitation because acoustics is dependent on that. A low frequency (< 100 Hz) has no directivity (diffraction), and as the frequency increases, the directional action becomes more and more significant. This will be quantified in the next section.

The directional effect is not considered in our simple method. The theoretical noise evaluated by quasi-steady theory will give a rough estimate (± 5 dB) of the noise at a distance of 2 m from the reactor. That value is the mean value between maximum and minimum induced by the directional effect.

6. TEST RESULTS

In order to validate our simple method, as well as trying to point out dynamic effects, we have tested a single core reactor at different frequencies, current, and measured the noise at different locations

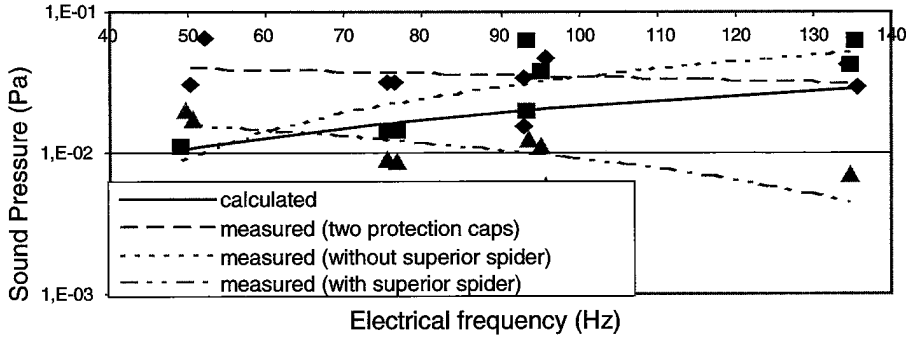

Figure 11. Sound pressure at 2 m from the reactor wall, for different cases. All cases are with the same nominal current of 80 A_{rms}.

around the apparatus and from close to far from it. Moreover, anti-noise protection ideas have been tested. The same test has also been performed with and without spiders.

Figure 11 shows the noise generated by the reactor both at 2 m from it and for a given point in the frequency domains of the tests. The curves clearly show different behavior. Some rough fittings are also indicated. The ordinates are logarithmic and give the rms pressure levels as predicted by our theory (straight line) and as measured on site.

It is quite interesting to note on Figure 11 that two cap protections (one on the top and one on the bottom) increase the noise in most of the frequency domains. This is probably because both caps were fixed on the reactor using spiders. So these caps move, due to both the axial reactor movement and the spiders' movement in the vertical plane. These movements induce speed on the caps, which offer a large surface favorable to noise generation, that is, a kind of music 'baffle' .... Future tests will be performed using such caps by suppressing contact with the reactor.

Figure 12 shows the noise generated by the reactor at 2 m from it and for two orthogonal positions around one quarter of the apparatus in the frequency domain.

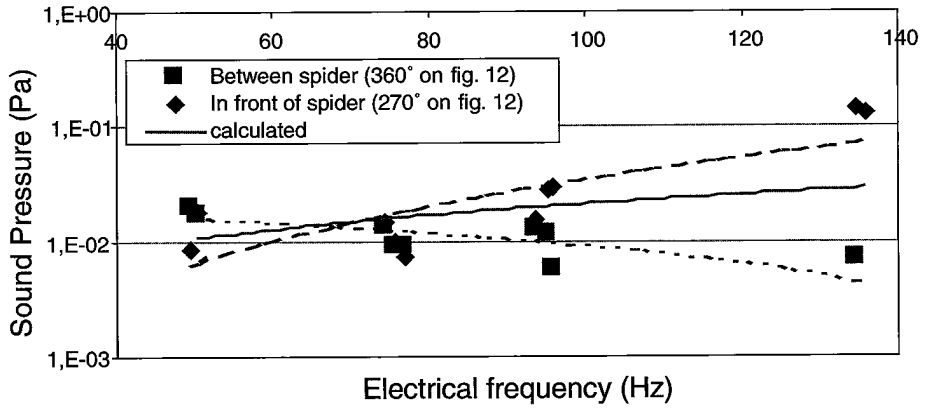

Figure 12. Sound pressure at 2 m around the reactor wall, clearly showing a directional effect.

It is quite clear (no disturbance in the curve) that no significant structural resonance or any acoustics resonance had occurred, despite the fact that tests were performed in the range of supposed resonance for some of them.

The simple quasi-steady theory gives a good rough estimation of the mean noise generated, neglecting the directional effect.

The directional effect can be as high as a 20 dB difference at electrical 150 Hz (acoustical mean, 300 Hz), but is negligible at 50 Hz, the basic electric case.

The noise level reduction with increasing frequency cannot be explained on a theoretical basis, but is still observed in some measurements. The only way to explain it is in relation with negative directional effect (in fact these measurements were done where speed compensation exists, in the front emitting surface). At low frequencies, such an effect does not exist because of diffraction in all directions. As the frequency increases, the directionality is more efficient and, as the closest emitting surface has lower speed, the measured noise at such a location could gradually decrease, but not of course in other locations around the cylinder. This is well observed in front of spiders, where amplification is significant. Quantifying the directional effect can be roughly deduced from Reference [3], and is about 5 dB at three times the frequency of no directional effect. So we maintain our basic theory and could specify the potential increase of that basic noise due to the unpleasant location.

If we remove the top spider, as seen on Figure 11, the result becomes very close to the theoretical approach, but with some overvalues because the bottom spider still exists and also induces some small swing due to insulator stiffness, which also creates directional effects.

But the basic case with top spider shows a significant difference with theory (Figure 12), which is now clearly stated as a directional effect. This is related to the fact that the measurement point for that figure was unfortunately chosen in front of a surface for which the speed was very limited.

7. ANTI-NOISE ACTIONS

Anti-noise actions can be taken as follows:

1. Limit wall speed: it is difficult to stiffen the reactor in radial direction; only both extremities could be stiffened by using more spiders. Copper is better than aluminium.
2. Design practice: the formula of the noise generated gives access to the design data of the reactor, which can be used to decrease the noise. However, few of them can really be adapted because they are fixed by electrical properties needed for the main goal of the reactance [4].
3. Anti-noise protection (passive or active): here we are faced with a cost problem for active protection. Concerning passive protection, a concrete protection wall could be envisaged (expensive). We could avoid inner noise generation by caps on the reactor (keeping in mind thermodynamics). Caps must be installed with no connection to the reactor.
4. Limit reflections: use absorptive materials for ground surfaces.
5. We would suggest (but unfortunately did not test) using a passive protection wall made of fiberglass with two concentric walls. Between these two walls, horizontal and vertical separations would be used to create different sized boxes (each having a specific resonance frequency). These boxes (= Helmholtz resonators) would include some holes oriented towards the reactor. Helmholtz resonators may thus be used to annihilate (create out of phase noise) the few well-known frequencies generating noise [1,2].

8. CONCLUSIONS

A practical approach to evaluate the acoustic noise generated by air-power reactors is proposed, based on very simple quasi-steady approach. Comparisons with more sophisticated methods (finite elements method) are presented. Despite the fact that the numerical method may 'easily' solve the problem, taking into account both structural resonance and acoustic ones, the many uncertainties in structural data, actual fixation on site, acoustic effects of the environment (both in testing and in actual location) may lead to dramatic discrepancies between measured and calculated values. Many complexities have been studied to see if acoustics or structural resonances could induce different effects, but the conclusion to date is that the suggested simple method is good enough (and includes the extremely interesting fact that such a method clearly points out the separate effect of each parameter) to explain all measured cases and fits quite well in the range of plus or minus 5 dB from measured values. Caution must be taken in measurement due to directional effects that are clearly explained in the text. Trends for anti-noise design and passive protection are also given in the text.

9. LIST OF SYMBOLS

B	the magnetic induction field (Tesla)
C	factor to convert the axial field to the field on the conductor (Equation (4)).
c	the sound speed (340 m/second in standard conditions)
E	the equivalent elasticity modulus of combined aluminium wire and dielectric section, (N/m^2)
e	the thickness of the wall (m)
F	the electromagnetic forces (N/m)
H	the total height of the reactor (m), $H = nbr \times \phi$
I_{rms}	the root mean square value of the sinusoidal $i(t)$ current (A)
$i(t)$	current (A),
N	the number of turns per unit length, $N = nbr/H = 1/\phi$
nbr	the total number of turns
p	sound pressure (Pa)
Δp	sound pressure normal gradient (being null on the ground) (Pa/m^2)
R	is the radius of the cylinder (m)
rms	root mean square
S_{emission}	the core wall surface (external + internal) (m^2)
t	time (seconds)
v	the speed (three components), on the reactor wall, on the ground (m/second)
v_{rad}	the normal component (to the core) of the core wall speed (m/second)
v_{n}	air particle speed near surface emission (m/second)
W	The acoustic power (watts)
ω	pulsation (rad/second) (of the current, of the vibration of the core wall, ...)
ϕ	the mean thickness of one turn (m)
μ_0	the vacuum magnetic permeability (H/m)
Δ	the Laplacian operator (m^{-2})
ρ	the volumetric mass of air (about 1.2 kg/m^3)

ACKNOWLEDGEMENT

Laser vibrometry speed measurements were performed by Pr. J.Cl. Golinval from the University of Liège. Acoustic noise measurements were performed by CEDIA (J. Nemerlin and X. Kaiser) (same University) and acoustic numerical evaluation performed by FFT (Free Field Technologies, Louvain-la-Neuve, Belgium).

G. Pelzer, P-A. Monfils, and G. Lo Pizzo from ALSTOM are sincerely thanked for their active contributions in both scientific content and testing in the ALSTOM laboratory.

REFERENCES

1. Alster M. Improved calculation of resonant frequencies of Helmholtz resonators. *Journal of Sound and Vibration* 1972; **24**(1):63–85.
2. Noise and Vibration control engineering. *Principles and applications*, Leo L. Beranek, Istvan L. Vér (eds). John Wiley & Sons, Inc.: Cambridge, MA, 1992.
3. Morse PM, Ingard KU. Theoretical Acoustics. Princeton University Press: Princeton, NJ, 1968.
4. Hugh M Ryan. High Voltage Engineering and Testing. *IEE Power and Energy Series* 2001; **32**:310–314.

AUTHOR'S BIOGRAPHY

J.-L. Lilien was born in Liège, Belgium on May 24th, 1953. He received his degree in Electrical and Mechanical Engineering from the University of Liège in 1976 and his Ph.D. from the same University in 1984. He is presently a professor at the University of Liège, Department of Transmission and Distribution of Electrical Energy. His main area of interest concerns the effects of short-circuit mechanical effects and overhead line vibrations (galloping). He is the chairman of two CIGRE task forces. He has published over 80 technical papers and has participated in many symposia and international conferences. He is a member of AIM electrical association (Belgium) and an IEEE member too. He may be contacted at the following address: Prof. J.L. Lilien, University of Liège, Montefiore Institute, Sart Tilman B28, 4000 Liège, Belgium, Tel. +32-43662633 ; Fax: +32-43662998, e-mail: lilien@montefiore.ulg.ac.be, url: www.montefiore.ulg.ac.be/services/tde